Journal of Alloys and Compounds 507 (2010) 414–418

Contents lists available at ScienceDirect

Journal of Alloys and Compounds

journal homepage: www.elsevier.com/locate/jallcom

Design induced plastic deformation in Zr-based bulk metallic glass

N.H. Tariq[a,*], J.I. Akhter[b], B.A. Hasan[a], M. Javed Hyder[c]

[a] Powder Metallurgy Lab, Department of Chemical and Materials Engineering, Pakistan Institute of Engineering and Applied Sciences, P.O. Nilore, Islamabad 45600, Pakistan
[b] Physics Division, Pakistan Institute of Nuclear Science & Technology, P.O. Nilore, Islamabad, Pakistan
[c] Department of Mechanical Engineering, Pakistan Institute of Engineering and Applied Sciences, P.O. Nilore, Islamabad, Pakistan

ARTICLE INFO

Article history:
Received 23 May 2010
Received in revised form 27 July 2010
Accepted 29 July 2010
Available online 4 August 2010

Keywords:
Bulk metallic glasses (BMGs)
X-ray diffraction (XRD)
Scanning electron microscope (SEM)
Compression test

ABSTRACT

In this study, effect of sample geometry on the mechanical properties of a Zr-based bulk metallic glass was investigated. For this purpose truncated conical samples with different semi-vertex angles (α) were prepared for quasistatic compression test. It was noticed that as the geometry of the sample was slightly deviated from a cylindrical shape (for which $\alpha = 0^\circ$) to a conical shape (for which $\alpha > 0^\circ$), stress gradients were induced in the conical samples which were estimated using finite element analysis. This led to the formation of a large amount of intersecting multiple shear bands. As a result, as-cast BMG sample with negligible plasticity tends to deform in a ductile manner.

1. Introduction

Bulk metallic glasses (BMGs) have immense potential applications as structural and functional materials owing to their superior properties like high strength, elastic deformability and corrosion resistance [1–3]. However, BMGs often show brittleness at room temperature. This still remains one of the most serious problems limiting their real engineering applications [4,5]. The localized inhomogeneous deformation in BMGs is the main cause of this brittleness. Upon yielding, nucleation of primary shear bands occurs preferentially in the direction of maximum shear stress and plastic deformations are highly confined to a small area in these bands. Hence, failures of BMGs occur catastrophically on one dominant shear band [6]. Recently, various strategies have been adopted to avoid rapid propagation of shear bands and to generate multiple shear bands by confining the sample geometrically [7–15]. In this work, truncated conical specimens of $Zr_{57.5}Cu_{11.2}Ni_{13.8}Al_{17.5}$ BMG with specific dimension were prepared for compression tests to investigate the effect of sample geometry. Under this design, due to geometrical constraints, a large amount of multiple shear bands were generated in the truncated conical BMG (TCB) samples [15]. This led to a considerable plastic displacement in TCB samples before failure. To substantiate the effect of the taper angle on the experimental results, particularly the stress distributions within the specimen, finite element analysis (FEA) was performed using ANSYS 10.0. Numerical simulation was carried out by constructing a 3-D model which precisely maps the sample geometry according to the actual parameters of different specimens of $Zr_{57.5}Cu_{11.2}Ni_{13.8}Al_{17.5}$ BMG used in this work. It is anticipated that the findings of this work would be very useful for future engineering applications of BMGs.

2. Experimental

Multi-component Zr-based BMG cylinder of nominal composition $Zr_{57.5}Cu_{11.2}Ni_{13.8}Al_{17.5}$ with dimensions ⟨Ø⟩ 3 mm × 50 mm was prepared by arc melting the mixtures of ultrasonically cleaned high purity Zr, Cu, Ni and Al metals. The detail of synthesis can be found elsewhere [15]. The rod was machined to produce truncated conical samples with dimensions and conical geometry as shown in Fig. 1. In order to investigate thermal parameters for the alloy Differential Scanning Calorimetry (DSC) was performed using TA INSTRUMENTS/DSC-Q100 at heating rate of 20 K/min. X-ray diffraction (XRD) of the alloy was conducted, by Shimadzu XRD-6000 using CuKα_1 radiation ($\lambda = 1.54060$ Å) to confirm the amorphous nature of the alloy. Compression test was conducted under uniaxial compressive quasistatic loading at constant strain rate of $4.2 \times 10^{-4}\,s^{-1}$ using specially designed conical samples with aspect ratio of 2. Finally, fractured surfaces of compression tested samples were examined by scanning electron microscope (SEM).

3. Results and discussion

XRD pattern of as-cast sample is given in Fig. 2 showing a halo region which is indicative of an amorphous structure. DSC plot of the alloy at heating rate of 20 K/min is shown as an inset of Fig. 2.

* Corresponding author. Tel.: +92 51 2207381/2207382; fax: +92 51 2208070.
E-mail address: naeem421@hotmail.com (N.H. Tariq).

0925-8388/$ – see front matter © 2010 Elsevier B.V. All rights reserved.
doi:10.1016/j.jallcom.2010.07.202

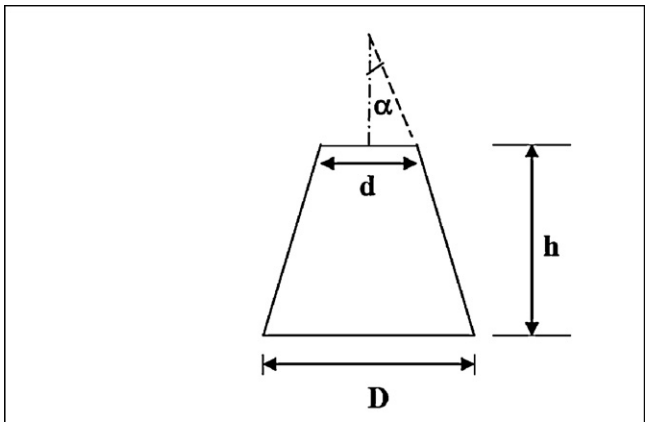

Sample Designation	d (mm)	D (mm)	h (mm)	α (deg.)
Sample 1 (Cylinderical)	3	3	6	0
Sample 2 (Conical)	2.5	3	6	2
Sample 3 (Conical)	2	3	6	5

Fig. 1. Geometry and dimensions of conical BMG samples.

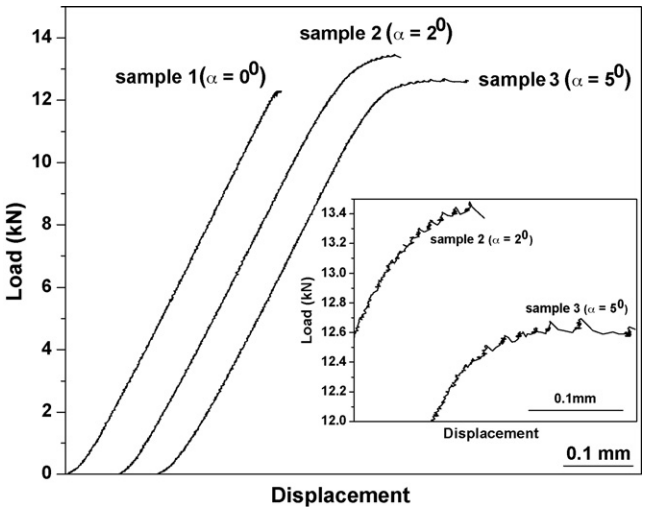

Fig. 3. Room temperature load–displacement curves for the alloy of different dimensions.

DSC trace exhibits a single endothermic peak, indicating the glass transition T_g, and an exothermic peak showing single stage crystallization reaction in the alloy. This also confirms amorphous nature of the alloy. Fig. 3 shows load–displacement curves for as-cast cylindrical specimen and conical samples with semi-vertex angle (α) of 2° and 5°. Fig. 3 reveals that the as-cast $Zr_{57.5}Cu_{11.2}Ni_{13.8}Al_{17.5}$ BMG sample with conventional cylindrical geometry fractured at the load of 12.3 kN after showing negligibly small plasticity. The fracture angle of sample 1 was measured to be 43°. On the other hand TCB samples showed distinct mechanical response. They exhibited considerable plasticity and also had increased fracture strength. The conical sample with $\alpha = 2°$ yielded at load of 12.1 kN. After yielding, the alloy showed displacement of about 0.1 mm and then fractured at load of 13.4 kN with fracture angle of 42°. In case of sample 3 with $\alpha = 5°$ yielding started at load of 11.2 kN. After yielding, the alloy showed displacement of about 0.2 mm and finally fractured at the load of 12.6 kN with fracture angle of 42.5°. It was also noted that load–displacement curve of conical samples exhibited flow serrations soon after yielding as shown in the inset of Fig. 3 with a magnified view. This serrated characteristic indicates simultaneous operation of multiple shear bands in contrast to a discrete shear band nucleation [14–16].

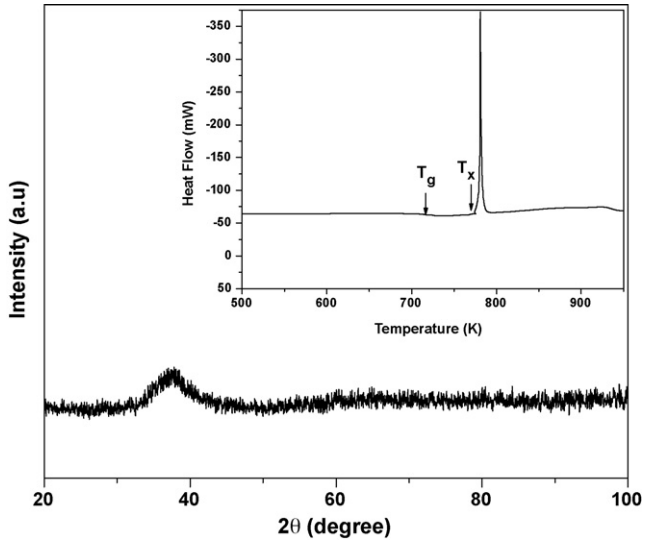

Fig. 2. XRD pattern of as-cast bulk amorphous alloy, inset shows DSC curve at heating rate of 20 K/min.

In order to understand the effect of the semi-vertex angle (α) on the stress distributions within the specimen, FEA was performed using ANSYS 10.0. For this purpose a 3-D model was constructed by precisely mapping the geometry of different specimens of $Zr_{57.5}Cu_{11.2}Ni_{13.8}Al_{17.5}$ BMG used in this work and numerical simulation was carried out. Von Mises stress distributions of sample with three different geometries in early stage (at total crosshead displacement of 0.04 mm) are shown in Figs. 4–6. Fig. 4 shows nearly uniform Von Mises stress distribution in cylindrical sample 1 with very small stress gradient indicating the end effect resulting from the interface between the crosshead and the specimen. On the other hand, conical samples with semi-vertex angle (α) of 2° (sample 2) and 5° (Sample3) show higher stress gradients as evident by stress contours in Figs. 5 and 6. High stress gradients in the conical samples lead to the evolution and interaction of multiple shear bands [14]. This is also apparent from the presence of flow serrations in the load–displacement curves of conical samples in Fig. 3.

Fig. 7(a) shows SEM image of the top view of fractured surface of sample 1 after compression test indicating a typical vein like morphology oriented in the same direction [15,17]. Formation of few non-interacting shear bands (marked by arrows) was also observed on the flat side of the fractured surface as shown in Fig. 7(b). Due to the formation of these few shear bands, sample 1 exhibited limited plasticity and fractured catastrophically by one dominant shear band [18]. SEM image of fractured surface of sample 2 is shown in Fig. 8(a) indicating distortion in the vein like morphology. Fig. 8(b) shows multiple and branched shear bands on the inclined side of the fractured surface of sample 2. The flow serrations of load–displacement curve of sample also support the presence of intersecting shear bands. Presence of stress gradients in the conical samples (Figs. 5 and 6) impedes the propagation of individual shear bands by promoting the multiplication and cross linking of the shear bands [12–15]. This results in the extensive improvement of plasticity. Fig. 9(a) shows SEM image of fractured surface of sample 3 indicating extreme distortion and branching of veins. It is quite interesting that with increasing semi-vertex

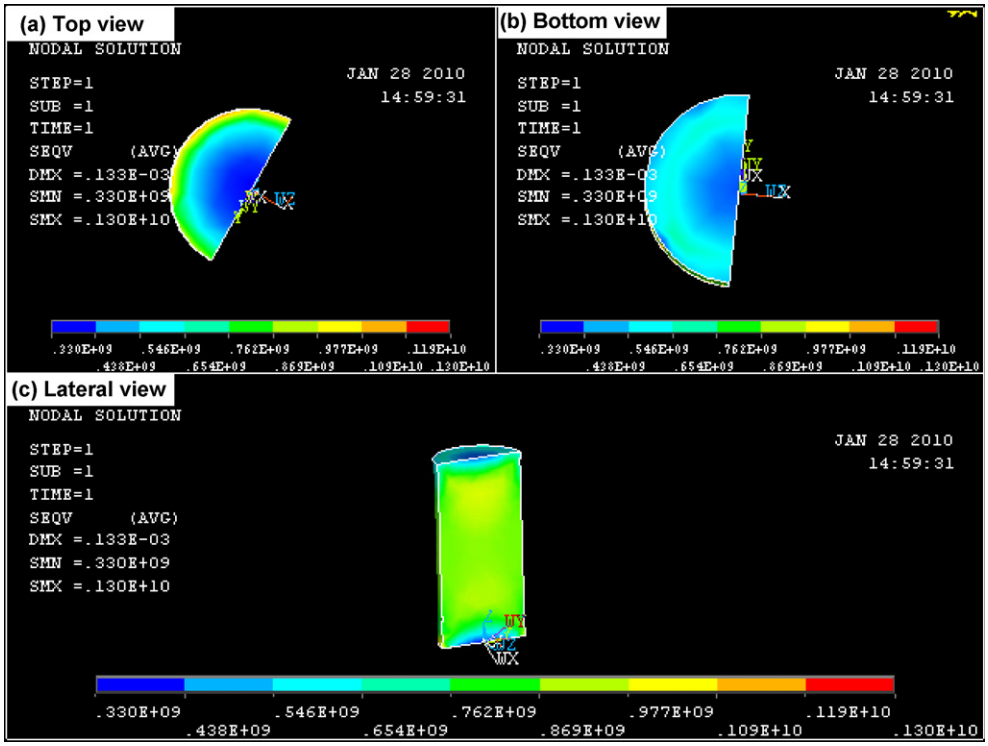

Fig. 4. Von Mises stress distribution in sample 1 under compression loading, top view (a), bottom view (b) and lateral view (1/2 portion) (c).

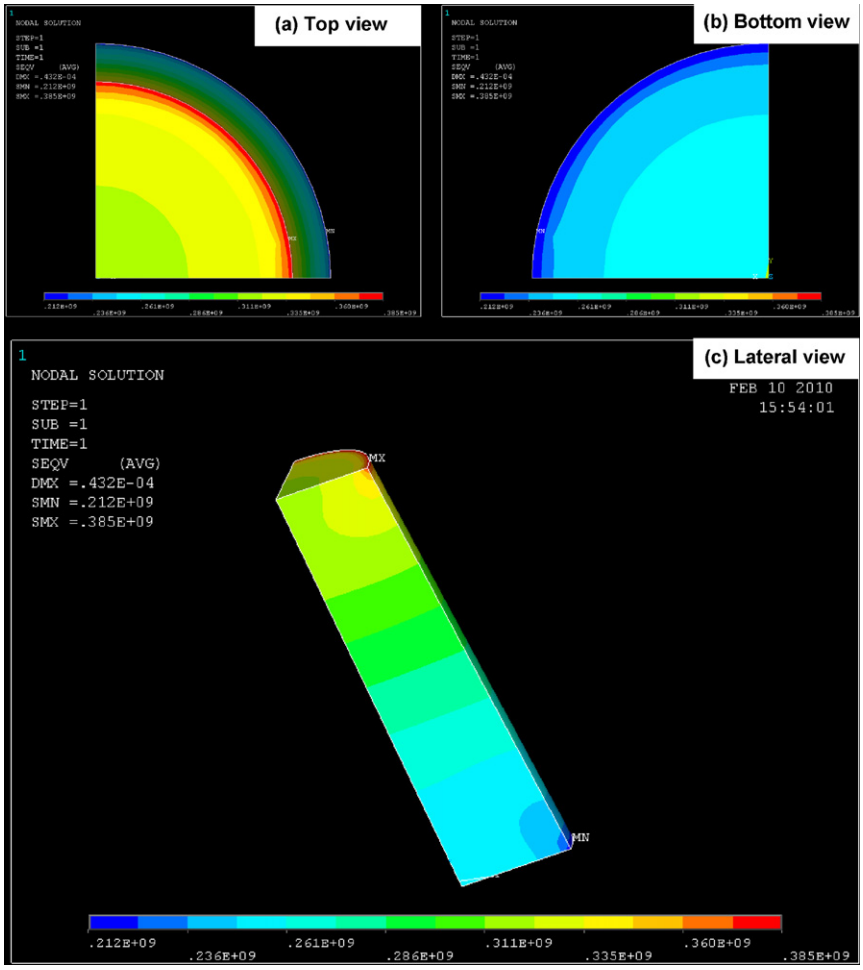

Fig. 5. Von Mises stress distribution in sample 2 under compression loading, top view (a), bottom view (b) and lateral view (1/4th portion) (c).

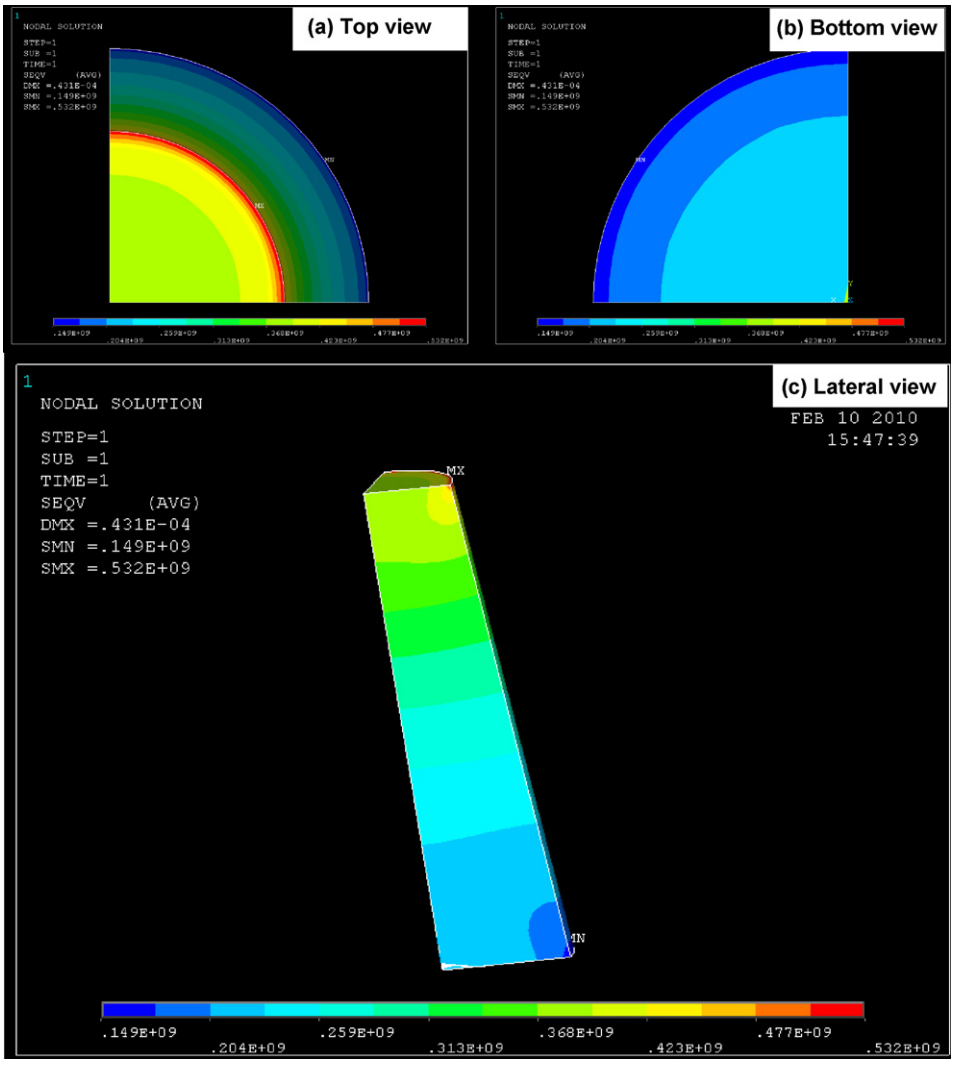

Fig. 6. Von Mises stress distribution in sample 3 under compression loading, top view (a), bottom view (b) and lateral view (1/4th portion) (c).

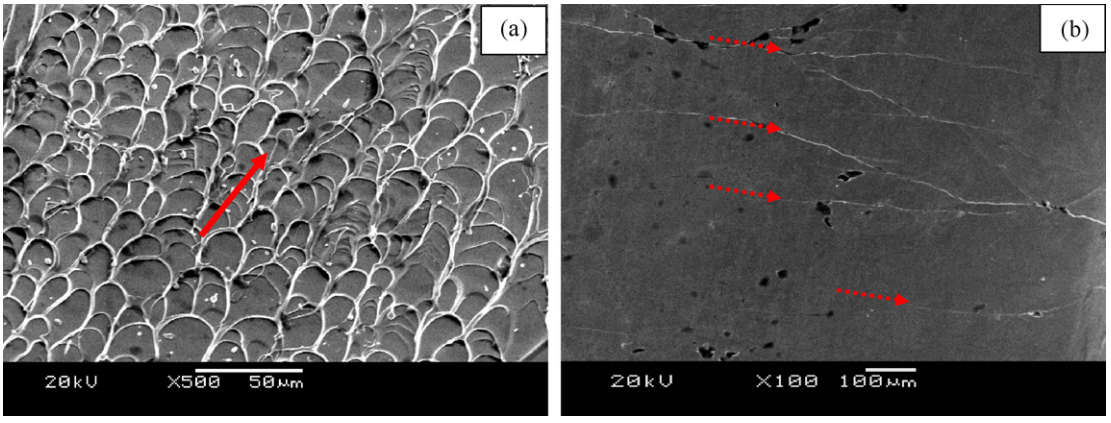

Fig. 7. SEM image of fractured surface of sample 1 showing typical vein like pattern elongated in the same direction (a). SEM micrographs of flat side of fractured surface showing few parallel shear bands (b).

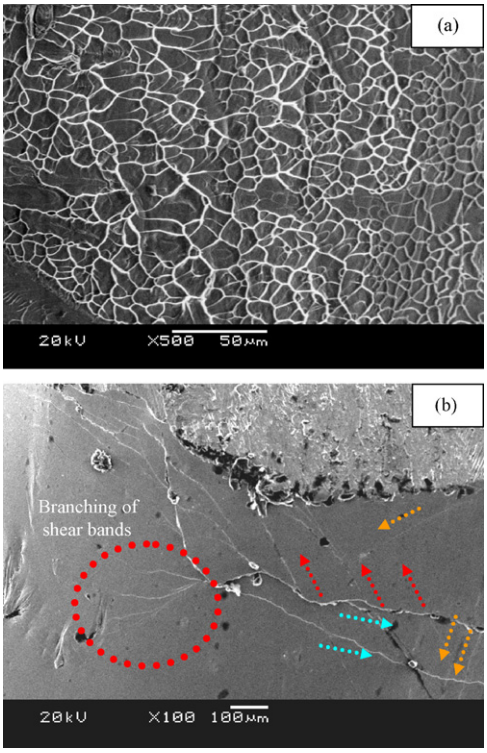

Fig. 8. SEM image of fractured surface of sample 2 showing distortion of veins (a). SEM micrographs of inclined side of fractured surface showing intersection and branching of shear bands (b).

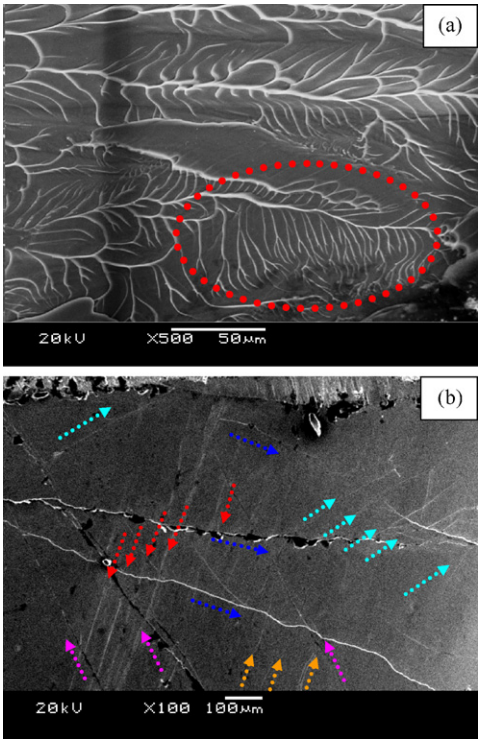

Fig. 9. SEM micrographs of fractured surface of sample 3 showing extreme distortion and branching of veins network (a). SEM micrographs of inclined side of fractured surface showing complex intersection of multiple shear bands (b).

angle (α) of conical sample from 2° to 5°, more effective geometrical confinement took place in the sample. As a result, a complex multi-axial stress state was induced in the sample that led to the extensive generation of multiple shear bands intersecting in a complex manner as shown in Fig. 9(b). This is also evident from the presence of few loops [5], secondary and tertiary branching of distorted veins (as circled in Fig. 9(a)) [15]. This shows that with a slight change in the geometry of the sample, i.e. from cylindrical shape (for which $\alpha = 0°$) to conical shape (for which $\alpha > 0°$), a BMG sample with limited plasticity, tends to deform in a ductile fashion. This change in deformation mode is merely attributed to the geometrical constraint (conical shape) induced complex stress distribution in the sample. This further led to the extreme distortion and branching of shear veins as well as evolution of complex intersecting multiple shear bands that avoid the undesired catastrophic failure. The present findings might be very useful from the perspective of engineering applications of BMGs. Since the change in sample geometry has shown very useful effect on the fracture behavior of the BMG with intrinsic negligibly small plasticity.

4. Conclusions

The specimen geometry strongly influences the deformation behavior of as-cast Zr-based BMG. As the geometry of the sample was changed from cylindrical shape to conical shape, BMG sample with negligibly small plasticity tends to deform in a ductile manner. This is due to the geometrical constraint induced complex stress distribution in TCB samples as estimated by FEA. The change in geometry further led to the evolution of complex intersecting multiple shear bands helpful for avoiding the catastrophic failure.

Acknowledgement

The authors are very thankful to Mr. Atique Ahmad of DME, PIEAS for providing technical support during the course of numerical simulation of this work.

References

[1] A.L. Greer, Science 267 (1995) 1947.
[2] A. Inoue, Acta Mater. 48 (2000) 279.
[3] N.H. Tariq, M. Iqbal, M.A. Shaikh, J.I. Akhter, M. Ahmad, G. Ali, Z.Q. Hu, J. Alloys Compd. 460 (2008) 258.
[4] W.L. Johnson, MRS Bull. 24 (1999) 42–56.
[5] N.H. Tariq, B.A. Hasan, J.I. Akhter, M.A. Shaikh, J. Alloys Compd. 477 (2009) L8.
[6] L. He, M.B. Zhong, Z.H. Han, Q. Zhao, F. Jiang, J. Sun, Mater. Sci. Eng. A 496 (2008) 285–290.
[7] H. Bei, S. Xie, E.P. George, Phys. Rev. Lett. 96 (2006) 105503.
[8] H.A. Bruck, T. Christman, A.J. Rosakis, W.L. Johnson, Scr. Metall. Mater. 30 (1994) 429.
[9] J.J. Lewandowski, P. Lowhaphandu, Philos. Mag. A 82 (2002) 3427.
[10] J. Lu, G. Ravichandran, J. Mater. Res. 18 (2003) 2039.
[11] Z.F. Zhang, H. Zhang, X.F. Pan, J. Das, J. Eckert, Philos. Mag. Lett. 85 (2005) 513.
[12] W.H. Jiang, G.J. Fan, H. Choo, P.K. Liaw, Mater. Lett. 60 (2006) 3537–3540.
[13] S. Xie, E.P. George, Intermetallics 16 (2008) 485–489.
[14] W.F. Wu, C.Y. Zhang, Y.W. Zhang, K.Y. Zeng, Y. Li, Intermetallics 16 (2008) 1190–1198.
[15] N.H. Tariq, J.I. Akhter, B.A. Hasan in press, doi:10.1007/s10853-010-4707-x.
[16] K.F. Yao, C.Q. Zhang, Appl. Phys. Lett. 90 (2007) 0619001.
[17] N.H. Tariq, B.A. Hasan, J.I. Akhter, F. Ali, J. Alloys Compd. 469 (2009) 179–185.
[18] F. Spaepen, Acta Metall. 25 (1977) 407.